EXPANSION OF A GAS CAVITY IN A GAS- AND WATER-SATURATED ELASTOPLASTIC MEDIUM

E. E. Lovetskii, A. M. Maslennikov,
and V. S. Fetisov

UDC 534.222

Experimental and theoretical research shows that the presence of gas and liquid in rocks has a considerable effect on the dynamics of the expansion of an underground cavity resulting from an underground explosion. Using his water head model Butkovich [1] investigated the influence of water on mechanical effects of powerful underground explosions. It was established that an increase in the amount of water in rock leads to an appreciable increase of the peak pressures at a compression wave front. The expansion of a cavity in a gas- and water-saturated medium was studied in [2] neglecting strength effects. Experiments [3] show that a correct theoretical description of the explosion process requires taking account of the elastoplastic properties of a gas- and water-saturated medium. In the present paper we present a numerical solution of the problem of the expansion of an underground cavity in a gas- and water-saturated elastoplastic medium as the result of an underground explosion.

1. Suppose at time zero an amount of energy W is liberated instantaneously in an explosion in a spherical cavity of radius R_0 in a multicomponent medium. We assume that the material in the cavity is an ideal gas with an adiabatic exponent $\gamma=1.4$. In general the adiabatic exponent changes during the expansion of the cavity, but we neglect this change and focus our attention mainly on the qualitative behavior of the multicomponent medium during the explosion. We describe the spherically symmetric motion of the medium by the hydrodynamic equations, taking account of strength effects. The initial equations in Lagrangian variables have the form

$$\begin{gathered}\partial v/\partial t = v\{\partial u/\partial r + 2u/r\},\\ \partial u/\partial t = v\{\partial \sigma_r/\partial r + 2\tau/r\},\\ \partial e/\partial t + p\partial v/\partial t = (2/3)\tau\{\partial u/\partial r - u/r\}.\end{gathered} \tag{1.1}$$

The first of Eqs. (1.1) is the equation of continuity, the second is the equation of motion, and the third is the energy equation. Here v and e are the specific volume and specific energy of the multicomponent medium, v_0 is the initial specific volume, u is the velocity, σ_r and σ_φ are the radial and tangential components of the stress tensor, $\tau=\sigma_r-\sigma_\varphi$ is the shear stress, $p=-(1/3)\ (\sigma_r+2\sigma_\varphi)$ is the pressure, t is the time, and r is the Eulerian coordinate. The right-hand side of the last of Eqs. (1.1) is related to the work done by the forces of plastic deformation arising during the motion of the medium.

The system of equations (1.1) is completed by the elastoplastic relations and the equations of state. We describe the mechanical properties of the medium in the elastic range by Hooke's law

$$\partial\tau/\partial t = 2G(\partial u/\partial r - u/r), \tag{1.2}$$

where G is the shear modulus. In the plastic range we use the Tresca yield criterion

$$|\tau| = \sigma^* = \text{const}, \tag{1.3}$$

where σ^* is the yield stress. By describing the plastic properties of the medium within the framework of the ideal plasticity model (1.3) we do not take account of the phenomenon of dry friction which is characteristic of soils. However, taking account of the plastic properties of the material in the form (1.3) is very simple and enables us to develop the main qualitative regularities of the dynamics of a gas- and water-saturated medium.

To take account of the gas and moisture saturation of a medium we chose the approach developed in [2, 4] which takes account of the multicomponent medium by a model equation of state with equal pressures and temperatures in all components. The definitions of the total specific energy and the total specific volume for a mixture yield the following relations:

$$e = \sum_{i=1}^{3} R_i e_i, \quad v = \sum_{i=1}^{3} R_i v_i, \tag{1.4}$$

Moscow. Translated from Zhurnal Prikladnoi Mekhaniki i Tekhnicheskoi Fiziki, No. 1, pp. 137-142, January-February, 1979. Original article submitted January 5, 1978.

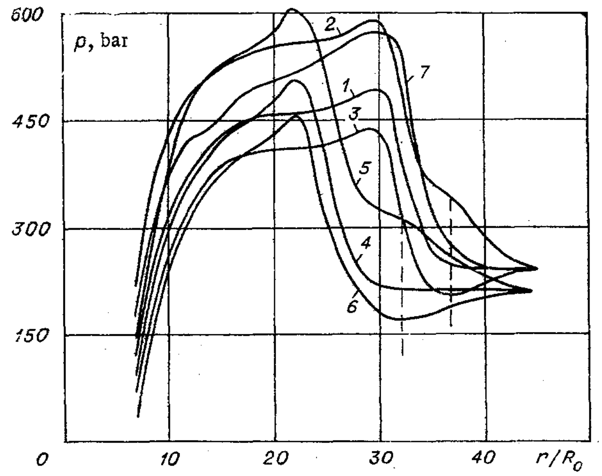

Fig. 1

where the R_i are the weight contents of the components (the subscript 1 corresponds to the solid component, 2 to water, and 3 to gas), the e_i are the specific internal energies, and the v_i are the specific volumes of the components. The equations of state of the solid and fluid components of the mixture were taken in the Mie–Gruneisen form [5]. The gas in the mixture was assumed ideal with $\gamma_1 = 1.7$.

Using the assumption of the equality of pressures in the components of the medium we neglect effects having characteristic times of the order of the time of the dynamic relaxation of stresses between components, which ordinarily does not exceed 10^{-4} sec. This assumption is justified since the characteristic times of the evolution of an explosion are longer than 10^{-3} sec. Our assumption of equal temperatures of the components is justified by the fact that according to [1] the characteristic times of equalizing temperatures is 10^{-5}–10^{-6} sec, which is shorter than the characteristic times of the evolution of an explosion. We assume that the expansion of the gas in the cavity is described by the same system (1.1) with $\sigma^* = 0$, and take as the equation of state the equation of state of an ideal gas with $\gamma = 1.4$. In this way we take account of the complex gasdynamic picture of the motion of the gas in the cavity. For the numerical solution the system of equations (1.1)–(1.4) was replaced by a system of difference equations approximating the initial system to second-order accuracy in Δt and Δr, where Δt and Δr are the sizes of the time and space nets. The hydrodynamic discontinuities in the difference equations were smoothed out by introducing a linear–quadratic artificial viscosity to ensure the possibility of a continuous solution. The stability of the calculation was ensured by an appropriate choice of the time step Δt. The pressure in the initial cavity and the initial values of p and e in the surrounding soil were specified. The velocity u at $t = 0$ was assumed zero everywhere. Boundary conditions were specified at the center ($r = 0$) and ahead of the shock front. A computer program was written for the difference equations and used to perform the numerical calculations.

2. Numerical calculations were performed for $G = 100$ kbar, $\sigma^* = 150$ bar, and $p_\Phi = 600$ bar, where p_Φ is the background pressure in the medium. In addition, calculations were performed with $\sigma^* = 0$ in order to find the influence of strength effects. The initial pressure in the cavity was 400 kbar in all the variations calculated. In the numerical calculations the values of R_2 and R_3 and the gas and water saturation of the soil were varied. The numerical calculations showed that for $t > 0$ a shock wave is propagated from the initial cavity boundary in the surrounding rock. Within the cavity a rarefaction wave travels through the gas to the center, is reflected back to the cavity wall, etc. From now on we do not discuss the behavior of the gas in the cavity since we are primarily interested in the behavior of the surrounding medium. Figures 1 and 2 show the radial distributions of pressure and the radial and tangential stresses for various values of the parameters at specified times. The dimensionless radius r/R_0 is plotted along the horizontal axis. Curves 1–3 represent p, σ_r, and σ_φ respectively for $R_1 = 0.9684$, $R_2 = 0.03$, $R_3 = 0.0016$ for $\lambda = t/t_0 = 32.5$, where $t_0 = R_0/\sqrt{Gv_0}$ (Fig. 1), and $\lambda = 70.0$ (Fig. 2). Curves 4-6 represent p, σ_r and σ_φ for $R_1 = 0.8968$, $R_2 = 0.1$, $R_3 = 0.0032$ for $\lambda = 32.5$ (Fig. 1) and $\lambda = 70.0$ (Fig. 2). Curve 7 shows the value of p calculated for $R_1 = 0.9684$, $R_2 = 0.03$, $R_3 = 0.0016$ for $\lambda = 32.5$ (Fig. 1) and $\lambda = 70.0$ (Fig. 2) for zero strength ($\sigma^* = 0$). This curve is shown for comparison. It is clear that an elastic precursor is propagated in front of the shock wave whose front can be identified with the position of the maxima. The presence of the elastic precursor leads to the sharp bend in the curves for $\sigma_r(r)$ (Fig. 1, curves 2 and 5). By using a linear–quadratic artificial viscosity the discontinuities are smoothed out. Therefore one can speak of an elastic precursor only qualitatively, since its radial profile is determined by a pseudoviscosity. Calculations show that to the right of the vertical dashed line the material is loaded elastically in

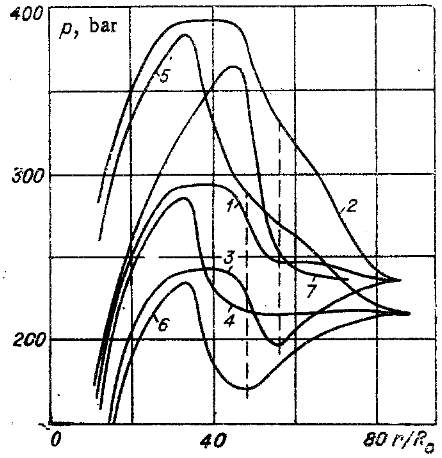

Fig. 2

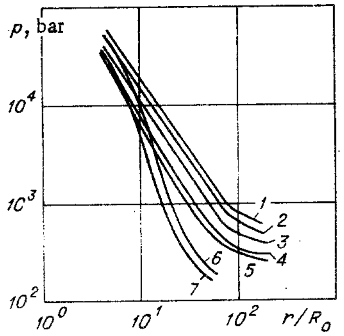

Fig. 3

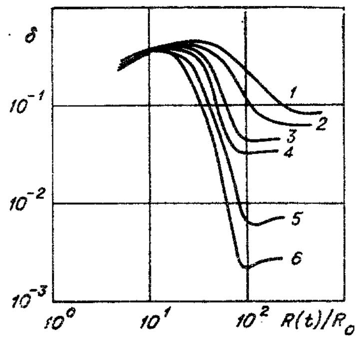

Fig. 4

accord with Eq. (1.2). Then plastic flow begins and continues up to the maximum value of the curves. After the pressure reaches its peak value the unloading of the material is at first elastic. Beyond the range of elastic unloading the material is unloaded plastically. Figure 3 shows the distribution of peak pressures as a function of r/R_0. Curve 1 corresponds to $R_1=1$, $R_2=0$, $R_3=0$; 2) $R_1=0.99$, $R_2=0.01$, $R_3=0$; 3) $R_1=0.97$, $R_2=0.03$, $R_3=0$; 4) $R_1=0.9$, $R_2=0.1$, $R_3=0$; 5) $R_1=0.85$, $R_2=0.15$, $R_3=0$; 6) $R_1=0.9968$, $R_2=0$, $R_3=0.0032$; 7) $R_1=0.991$, $R_2=0$, $R_3=0.009$. We note that the porosity of the material for curves 2 and 6 and for 3 and 7 is the same. A small difference in weight contents of water and gas (the latter approximately one-third as large) involves an appreciable background pressure ($p_\Phi=200$ bar). Figure 3 shows that the peak pressures in the loading wave decrease sharply with an increase in moisture content. Replacing water by gas leads to a still stronger damping of the shock wave. The results obtained are in qualitative agreement with the results in [2]. The sharper change in the character of the damping of the peak stresses with an increase in gas and water content noted in [2] results from the fact that the calculations in [2] were performed for zero back pressure. The log–log plots in Fig. 3 show that the peak pressures vary as a power of the radius for $R_3=0$. The deviation of curves 1-5 from linearity for large r results from the transformation of the shock wave into an elastic wave.

The curves in Fig. 4 characterize the ratio of the total kinetic energy of all the moving material to the total energy of the explosion ($\delta=e_k/W$) as a function of the position of the boundary of the material disturbed by the motion $R(t)/R_0$. Curves 1-6 correspond to the following gas and water contents: 1) $R_1=1$, $R_2=0$, $R_3=0$; 2) $R_1=0.97$, $R_2=0.03$, $R_3=0$; 3) $R_1=0.9$, $R_2=0.1$, $R_3=0$; 4) $R_1=0.85$, $R_2=0.15$, $R_3=0$; 5) $R_1=0.9968$, $R_2=0$, $R_3=0.0032$; 6) $R_1=0.991$, $R_2=0$, $R_3=0.009$. The results can be interpreted in the following way. Initially the value of δ increases, and in this stage there is a transformation of the energy of the gas in the cavity to kinetic energy of the surrounding medium. As the multicomponent medium is set in motion there is a dissipation of energy both in the shock transition and in plastic flow. Therefore the parameter δ is always much smaller than unity. From a certain instant the dissipation process begins to predominate over the pumping of energy from the cavity. As a result the kinetic energy of the moving medium begins to decrease as the shock wave is propagated. Finally, for $R(t)/R_0 > 100$ all the curves have constant asymptotes. This is related to the end of plastic flow; further motion is elastic. In the proposed model there is no dissipation of energy in the elastic region, which leads asymptotically to a constant value of δ. It is clear that this asymptotic value of δ is smaller the larger the water content (curves 1-4). For zero water content (curves 5, 6) the asymptotic value of δ decreases with increasing gas content. Thus the higher the gas content, i.e., the higher the compressibility of

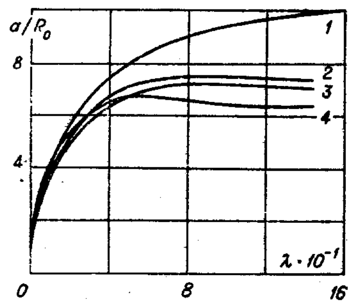

Fig. 5

the multicomponent medium, the smaller is the fraction of the energy of the explosion transformed into energy of elastic waves and residual elastic strains. Figure 5 shows the time dependence of the radius of the cavity $a(t)/R_0$ as a function of λ. Curve 1 corresponds to $\sigma^* = 0$, $R_1 = 0.9684$, $R_2 = 0.03$, $R_3 = 0.0016$; 2) $R_1 = 1$, $R_2 = 0$, $R_3 = 0$; 3) $R_1 = 0.85$, $R_2 = 0.15$, $R_3 = 0$; 4) $R_1 = 0.991$, $R_2 = 0$, $R_3 = 0.009$. For zero strength (curve 1) the final maximum size of the cavity is determined solely by the back pressure p_Φ. The final size of the cavity decreases with increasing compressibility (with an increase in water and gas content). This is evidently related to the increase in the dissipation of the energy of the explosion (cf. Fig. 4) with an increase in the gas and water saturation.

We note that in all the variations calculated the backward motion of the cavity did not exceed 5-7%. This result is in agreement with data in [6].

The numerical results presented above show the effect of a change in gas and water contents on an explosion in rock. For identical initial porosity the mechanical effect of an explosion increases with an increase in the water saturation of the rock. Replacing the gas in the pores by water leads to an appreciable increase in peak pressures at the shock front, a larger value of the energy radiated in elastic waves, and a larger size of the cavity. Physically this is related to the decrease in compressibility of the continuous medium with a decrease in gas content and a corresponding increase in water content. Analysis of the results of the calculation shows that taking account of strength effects determines the final size of the cavity. For $\sigma^* = 0$ the size of the cavity is appreciably larger than the corresponding size for $\sigma^* \neq 0$. The difference in values of the peak stresses is 20-25%. A consideration of the energy characteristics of the medium shows that the dissipation of energy of an explosion increases with increasing gas and water content.

LITERATURE CITED

1. T. R. Butkovich, "The influence of water in rocks on the effect of underground nuclear explosion," in: Underwater and Underground Explosions [in Russian], Mir, Moscow (1974).
2. G. M. Lyakhov and V. N. Okhitin, "Spherical blast waves in multicomponent media," Zh. Prikl. Mekh. Tekh. Fiz., No. 2 (1974).
3. Explosion Physics [in Russian], Nauka, Moscow (1975).
4. G. M. Lyakhov, Fundamentals of the Dynamics of Blast Waves in Soils and Rocks [in Russian], Nauka, Moscow (1974).
5. Ya. B. Zel'dovich and Yu. P. Raizer, Physics of Shock Waves and High-Temperature Hydrodynamic Phenomena, Academic Press, New York (1966).
6. V. A. Batalov and V. A. Svidinskii, "Investigation of the effects of the medium parameters on the final size of a cavity in a strong underground explosion," Izv. Akad. Nauk SSSR, Fiz. Zemli, No. 12 (1971).